ELSEVIER

Nuclear Instruments and Methods in Physics Research A 427 (1999) 353–356

NUCLEAR INSTRUMENTS & METHODS IN PHYSICS RESEARCH
Section A

The ray-tracing code Zgoubi

François Méot*

CEA/Saclay, DSM/DAPNIA/SEA, 91191 Gif-sur-Yvette Cedex, France

Received 14 April 1998; received in revised form 6 July 1998; accepted 3 November 1998

Abstract

The ray-tracing code Zgoubi computes particle trajectories in arbitrary magnetic and/or electric field maps or analytical models. The code is a genuine compendium of numerical recipes for simulation of most types of optical elements encountered in beam optics. It contains a built-in fit procedure, synchrotron radiation calculation, spin tracking, many Monte Carlo processes, etc. The high accuracy of the integration method allows efficient multiturn tracking in periodic machines. © 1999 Published by Elsevier Science B.V. All rights reserved.

Keywords: Ray-tracing; Spin; Synchrotron radiation; Tracking

1. Introduction

The ray-tracking code Zgoubi [1] (see also Ref. [2]) computes charged particle trajectories in arbitrary number, in arbitrary magnetic and/or electric field maps or analytical models of fields. The code is a genuine compendium of numerical recipes for simulation of most types and geometries of optical elements encountered in beam lines, spectrometers, and periodic machines. It contains a built-in fit procedure, synchrotron radiation calculation, spin tracking, in-flight decay and several other Monte Carlo process simulations, etc. The high accuracy of the method allowed efficient multiturn tracking in recent studies [3–5].

2. Integration of the Lorentz equation

The motion of a particle of charge q, mass m, and velocity $\boldsymbol{v}$ in electric and magnetic fields $\boldsymbol{e}$ and $\boldsymbol{b}$ is described by the Lorentz equation $\mathrm{d}(m\boldsymbol{v})/\mathrm{d}t = q(\boldsymbol{e} + \boldsymbol{v} \times \boldsymbol{b})$. Taking

$$\boldsymbol{u} = \frac{\boldsymbol{v}}{v}, \quad \mathrm{d}s = v\,\mathrm{d}t, \quad \boldsymbol{u}' = \frac{\mathrm{d}\boldsymbol{u}}{\mathrm{d}s}, \quad m\boldsymbol{v} = mv\boldsymbol{u} = qB\rho\boldsymbol{u},$$

where $B\rho$ is the rigidity of the particle, it can be rewritten under the more handy form $(B\rho)'\boldsymbol{u} + B\rho\boldsymbol{u}' = (\boldsymbol{e}/v) + \boldsymbol{u} \times \boldsymbol{b}$. From the position $\boldsymbol{R}$, unit velocity $\boldsymbol{u}$ and rigidity $B\rho$ at location M_0, the position, unit velocity and rigidity at M_1 following a displacement Δs (Fig. 1) are obtained from the truncated Taylor series

$$\boldsymbol{R}(M_1) = \boldsymbol{R}(M_0) + \boldsymbol{u}(M_0)\Delta s + \boldsymbol{u}'(M_0)\frac{\Delta s^2}{2!} + \cdots + \boldsymbol{u}'''''(M_0)\frac{\Delta s^6}{6!}$$

* *E-mail address:* fmeot@cea.fr (F. Méot)

PII: S0168-9002(98)01508-3

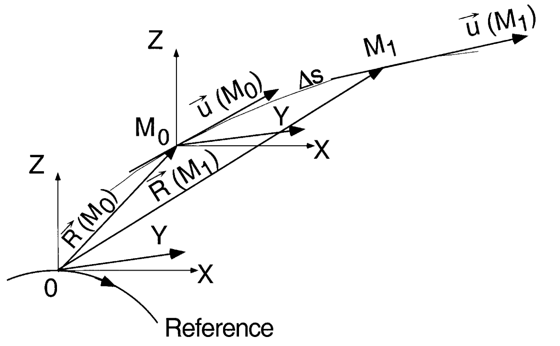

Fig. 1. Particle motion in the Zgoubi frame, and parameters used in the text.

$$\boldsymbol{u}(M_1) = \boldsymbol{u}(M_0) + \boldsymbol{u}'(M_0)\,\Delta s + \boldsymbol{u}''(M_0)\,\frac{\Delta s^2}{2!} + \cdots + \boldsymbol{u}'''''(M_0)\,\frac{\Delta s^5}{5!}$$

$$(B\rho)(M_1) = (B\rho)(M_0) + (B\rho)'(M_0)\Delta s + \cdots + (B\rho)''''(M_0)\,\frac{\Delta s^4}{4!}.$$

The derivatives $\boldsymbol{u}^{(n)} = \mathrm{d}^n\boldsymbol{u}/\mathrm{d}s^n$ involved in these expressions are obtained as functions of the derivatives $\boldsymbol{e}^{(n)}$, $\boldsymbol{b}^{(n)}$ and $(B\rho)^{(n)} = \mathrm{d}^n(B\rho)/\mathrm{d}s^n$, by recursive differentiations of the equation of motion, while the

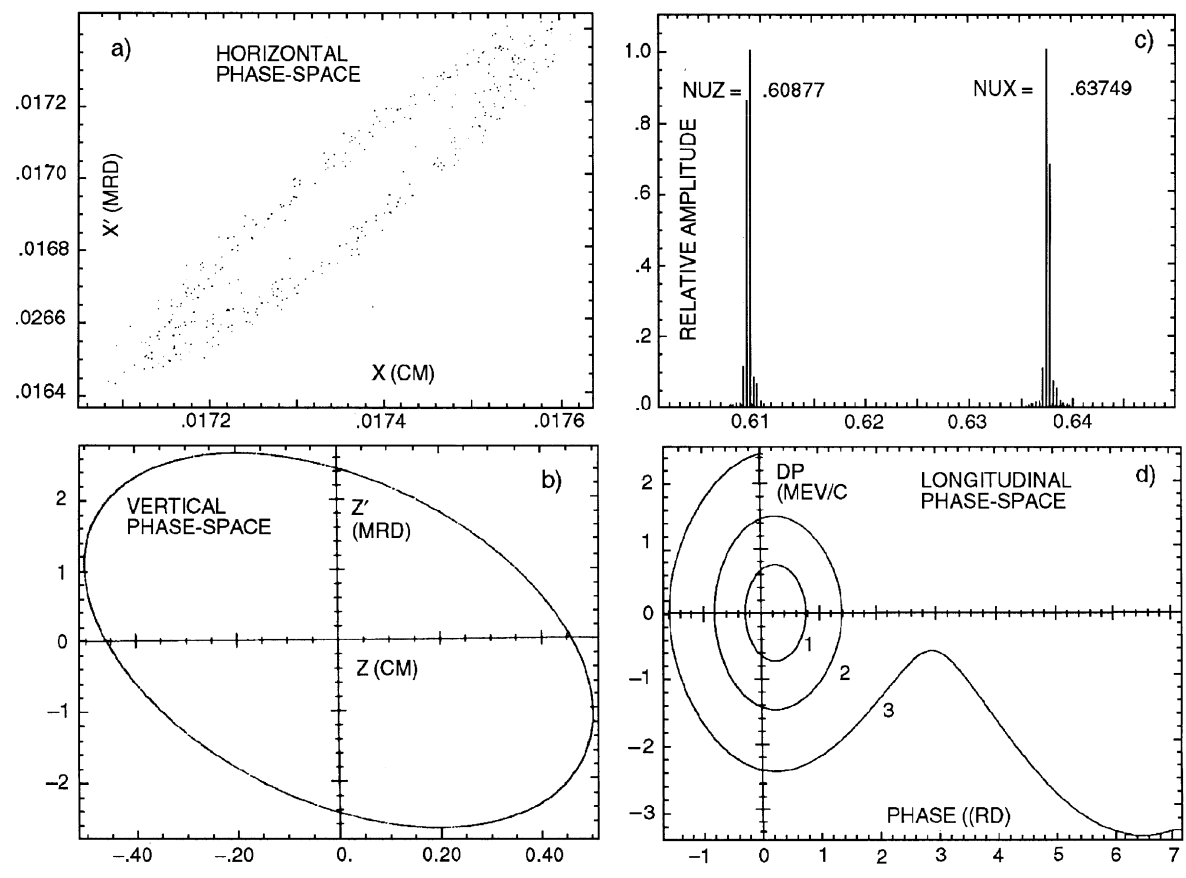

Fig. 2. Transverse phase spaces and related tunes, longitudinal phase space, obtained from 3000-turn single particle tracking in the SATURNE synchrotron (CEA-Saclay).

latter is obtained from alternate recursive differentiations of, on the one hand, $(B\rho)' = (1/v)(\boldsymbol{e}\cdot\boldsymbol{u})$ and on the other, $(1/v)' = (1/c^2)(\boldsymbol{e}\cdot\boldsymbol{u})/B\rho - (1/v)(B\rho)'/B\rho$. Finally, the fields $\boldsymbol{e}$ and $\boldsymbol{b}$ and their derivatives are explicitly provided by the code, from field maps and analytical models of optical elements.

The stringency of multiturn tracking makes it a very good test of the efficiency of the integration method and of such feature as symplecticity. This is illustrated in Fig. 2, which shows the negligible spread of transverse phase-space ellipses, and the perfect definition of the transverse tunes (obtained by Fourier analysis) and of the synchrotron motion.

3. Spin tracking

The motion of the spin $\boldsymbol{S}$ of a charged particle is governed by the Thomas-BMT equation [6] $\mathrm{d}\boldsymbol{S}/\mathrm{d}t = (q/m)\boldsymbol{S}\times\boldsymbol{\Omega}$ in which $\boldsymbol{\Omega} = (1+\gamma G)\boldsymbol{b} + G(1-\gamma)\boldsymbol{b}_{\|}$, γ is the Lorentz relativistic factor and G is the anomalous magnetic moment of the particle. $\boldsymbol{b}_{\|}$ is the component of $\boldsymbol{b}$ which is parallel to the velocity $\boldsymbol{v}$ of the particle. Using the notations of the previous section and introducing $\boldsymbol{\omega} = \boldsymbol{\Omega}/B\rho$, the Thomas-BMT equation transforms to the more convenient form $\boldsymbol{S}' = \boldsymbol{S}\times\boldsymbol{\omega}$. Given the values of the magnetic factor $\boldsymbol{\omega}$ and the spin $\boldsymbol{S}$ of the particle at location M_0, the spin at M_1 is obtained from

$$\boldsymbol{S}(M_1) = \boldsymbol{S}(M_0) + \frac{\mathrm{d}\boldsymbol{S}}{\mathrm{d}s}(M_0)\,\Delta s + \frac{\mathrm{d}^2\boldsymbol{S}}{\mathrm{d}s^2}(M_0)\frac{\Delta s^2}{2} + \frac{\mathrm{d}^3\boldsymbol{S}}{\mathrm{d}s^3}(M_0)\frac{\Delta s^3}{3!} + \frac{\mathrm{d}^4\boldsymbol{S}}{\mathrm{d}s^4}(M_0)\frac{\Delta s^4}{4!}.$$

The derivatives $\boldsymbol{S}^{(n)} = \mathrm{d}^n\boldsymbol{S}/\mathrm{d}s^n$ of $\boldsymbol{S}$ at M_0 are obtained by differentiating $\boldsymbol{S}' = \boldsymbol{S}\times\boldsymbol{\omega}$ while by projection, $\boldsymbol{b}_{\|} = (\boldsymbol{b}\cdot\boldsymbol{u})\boldsymbol{u}$ recursively differentiable.

Fig. 3 shows the crossing of the quadrupole resonance $\gamma G = 7 - \nu_z$ in SATURNE: curve (A) is obtained with an acceleration rate of $\mathrm{d}B/\mathrm{d}t = 2.1$ T/s, on the invariants $\varepsilon_y/\pi = 0$ and $\varepsilon_z/\pi = 1.22\times10^{-6}$ m rad, curve (B) is with $\varepsilon_z/\pi = 1.22\times$

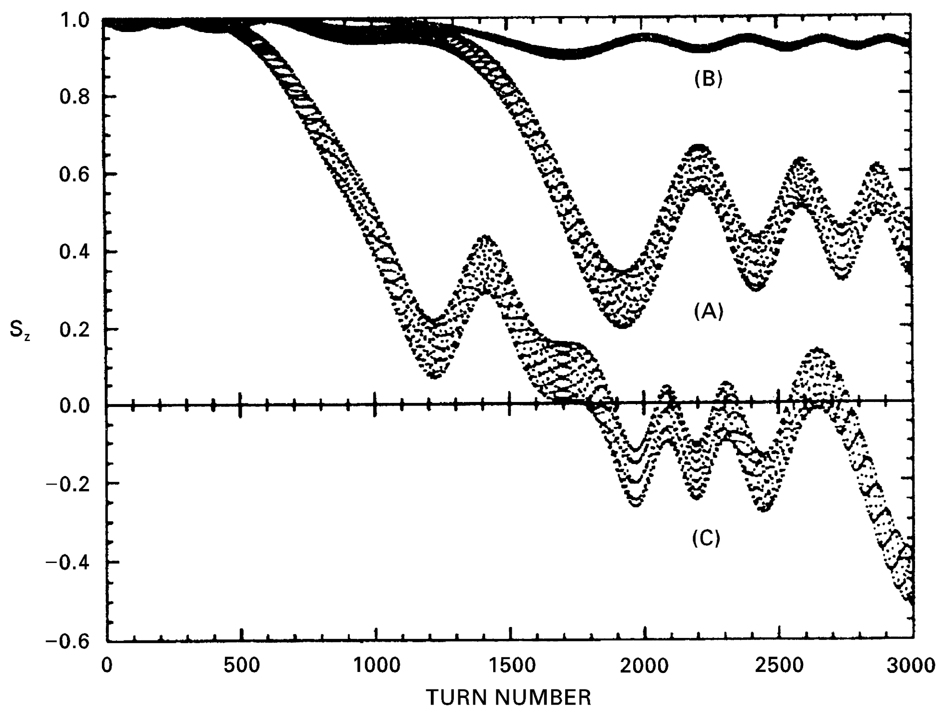

Fig. 3. Evolution of the vertical spin component S_z versus turn number at the traversal of the $\gamma G = 7 - \nu_z$ depolarizing resonance in SATURNE, in the case of a strong resonance (A), weak resonance (B), and in the presence of synchrotron motion (C).

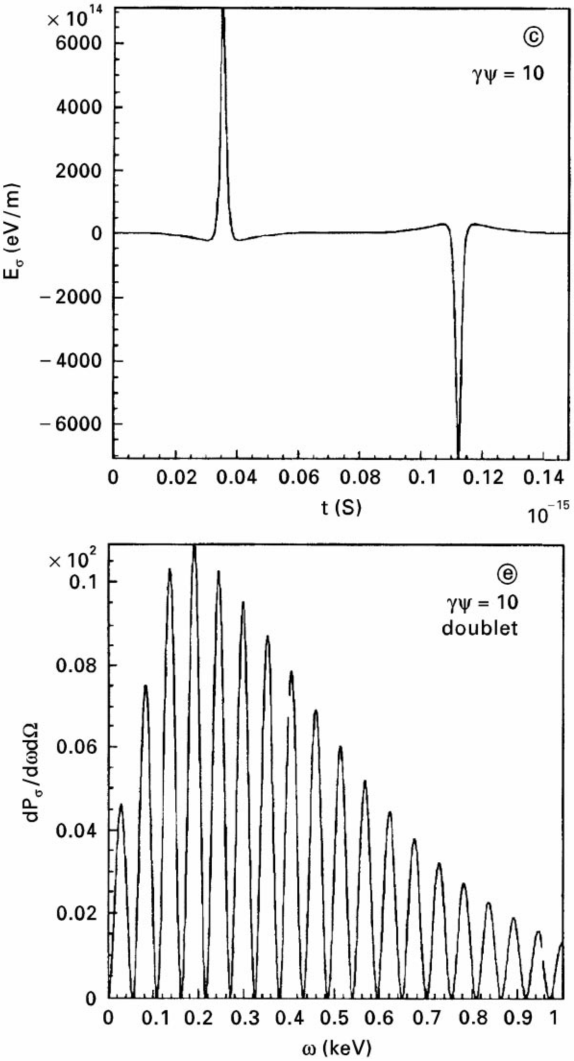

Fig. 4. The electric field component E_σ of the double impulse emitted in a pair of small dipoles observed under $\psi = 10/\gamma$ vertical angle (Fig. c), and the resulting interferential spectrum (Fig. e).

10^{-6} m rad, both in perfect agreement with standard analytical material [7]; the curve (C) cannot be attained with analytical means: it shows the behaviour of $S_z(t)$ for an off-momentum particle subject to synchrotron motion with a maximum amplitude $\delta p/p = 10^{-3}$.

4. Synchrotron radiation

The ray-tracing procedures described in Section 2 provide the ingredients necessary for the determination of the electric field radiated by the particle subject to acceleration in the far-field approximation, namely [8]

$$\mathscr{E}(\boldsymbol{n}, \tau) = \frac{q}{4\pi\varepsilon_0 c} \frac{\boldsymbol{n}(t) \times [(\boldsymbol{n}(t) - \boldsymbol{\beta}(t)) \times \mathrm{d}\boldsymbol{\beta}/\mathrm{d}t]}{r(t)(1 - \boldsymbol{n}(t) \cdot \boldsymbol{\beta}(t))^3}$$

where t is the particle time, τ is the observer time, $\boldsymbol{\beta} = \boldsymbol{v}/c$, $\boldsymbol{r}(t)$ is the distance from the particle to the observer and $\boldsymbol{n} = \boldsymbol{r}(t)/r(t)$. As an example Fig. 4 shows the two electric field impulses emitted by a single particle that crosses successively two neighbouring small magnets and the resulting interferential spectrum whose modulation depends on the distance between the magnets. The high degree of precision of the ray-tracing is revealed by the perfect agreement with theoretical material [9].

References

[1] D. Garreta, J.C. Faivre, First Version of Zgoubi, DPh-N, CEA-Saclay, 1972.
[2] F. Méot, S. Valéro, Zgoubi users' guide, Report CEA DSM/DAPNIA/SEA/97-13, and FERMILAB-TM-2010, December 1997.
[3] F. Méot, Part. Accel. 52 (1996).
[4] F. Méot, A. París, Report FERMILAB-TM-2017, August 1997.
[5] F. Méot, Report FERMILAB-TM-2016, August 1997.
[6] V. Bargmann, L. Michel, V.L. Telegdi, Phys. Rev. Lett. 2 (1959) 435.
[7] M. Froissard, R. Stora, Nucl. Instr. and Meth. 7 (1960) 297.
[8] J.D. Jackson, in: Classical Electrodynamics, Wiley, New York, 1975.
[9] F. Méot, Report CERN SL/94-22 (AP), 28 June 1994.